New Dual-Dielectric Gate All Around (DDGAA) RADFET Dosimeter Design to Improve the Radiation Sensitivity

F. Djeffal, T. Bendib, M. Meguellati, D. Arar and M.A Abdi

Abstract— **In this paper, a radiation sensitive FET (RADFET) dosimeter design (called the Dual-Dielectric Gate All Around DDGAA RADFET dosimeter) to improve the radiation sensitivity performance and its analytical analysis have been proposed for RADFET dosimeter-based applications (monitoring, robotics, medical sciences,…). Analytical models have been developed to predict and compare the performance of the proposed design and conventional (bulk) RADFET, where the comparison of device architectures shows that the proposed design exhibits a superior performance with respect to the conventional RADFET in term of fabrication process and sensitivity performances. In addition, Gentec Alg –based approach has been developed to optimize (maximization) the sensor sensitivity. The obtained results make the DDGAA RADFET dosimeter a promising candidate for future integrated CMOS-based dosimeters.**

Index Terms—**dosimeter, RADFET, traps, irradiation, sensitivity. Introduction**

THE Gate All Around GAA MOSFETs have emerged as excellent devices to provide the electrostatic integrity needed to scale down transistors to minimal channel lengths, and allowing a continuous progress in digital and analog applications. In addition to a better electrostatics than the conventional bulk MOSFET, the use of these devices have advantages relative to the electronic transport, mainly due to (i) the reduced surface roughness scattering because the lower vertical electric field and (ii) the reduction of the Coulomb scattering because the film is made of undoped/low-doped silicon [1-5]. Design and modeling guidelines of GAA MOSFETs have been discussed in previous work [2-5]. Employing this design for environment monitoring applications (irradiation measurement) becomes more beneficial if the device is made in vertical cylindrical recrystallized silicon due to highly flexible process integration options. There have been several reports of MOSFETs fabricated in recrystallized silicon for high-density digital integrated circuits [5].

Radiation sensitive MOSFETs (RADFETs) have been focus of interest both from applications and fundamental research point of views. In electronic industry these devices are considered as attractive alternatives for nuclear industry, space, radiotherapy and environment monitoring applications due to their reliability, low power consumption, non-destructive read-out of dosimetric information, high dose range, and compatibility to standard CMOS technology and on-chip signal processing [6-8]. The main RADFET disadvantage is the relatively low sensitivity. In this context, the submicron multi-gate design may be considered as attractive alternative to overcome this disadvantage because of the high electrical performance and reliability provided by the multi-gate structure in comparison with single-gate one. However, as semiconductor devices are scaled into the deep submicron domain, short-channel effects (SCEs) begin to plague conventional planar CMOS-based devices. To avoid the electrical constraints and improve the sensitivity performance, a new design and enhancement of conventional (bulk) RADFET become important. In this work, a new design of RADFET called the Dual-Dielectric Gate All Around (DDGAA) RADFET dosimeter, in which the manufacturing processes and sensitivity performances will be greatly improved, is proposed for deep submicron CMOS-based dosimeter applications. The (DDGAA) RADFET dosimeter design presented in this paper is basically surrounded dual-dielectric layers (SiO2 and Si3N4) with low p-channel (Si) doping concentration. The results showed that the analytical model is in agreement with the 2-D numerical simulation over a wide range of device parameters. The proposed structure has been analyzed and validated by the good sensitivity and electrical performance obtained in deep submicron regime in comparison with the conventional (bulk) design.

This paper is organized as follows. In Section 2, we derive an analytical interface potential distribution including radiation-induced interface-traps. The threshold voltage shift model can then be determined based on the interface potential model. In Section 3, we investigate the performance of the proposed design. The conclusions will be drawn in Section 4.

I. THEORY DEVELOPMENT AND MODEL DERIVATION

A. *Interface potential analysis*

Schematic cross-sectional view of the proposed (DDGAA) RADFET dosimeter is presented in Fig.1. The insulator consists of a thermal oxide (SiO_2) grown on a (100) n on n+ expitaxial silicon substrate (channel), and a low pressure CVD silicon nitride layer(Si_3N_4) deposited on top of the oxide. $N_{D/S}$ represents the doping level of the drain/source region, respectively. The channel region is bounded by source and

F. Djeffal is with the Laboratory of Advanced Electronic, Department of Electronics, LEPCM, University of Batna, 05000, Algeria (e-mail: faycaldzdz@ hotmail.com, Tel/Fax: 0021333805494).

T. Bendib is with the Laboratory of Advanced Electronic, Department of Electronics, University of Batna, 05000, Algeria (e-mail: bendib05.t@ gmail.com).

M. Meguellati is with the Laboratory of Advanced Electronic, Department of Electronics, University of Batna, 05000, Algeria (e-mail: M. Meguellati @ hotmail.com).

ISBN: 978-988-19252-1-3
ISSN: 2078-0958 (Print); ISSN: 2078-0966 (Online)

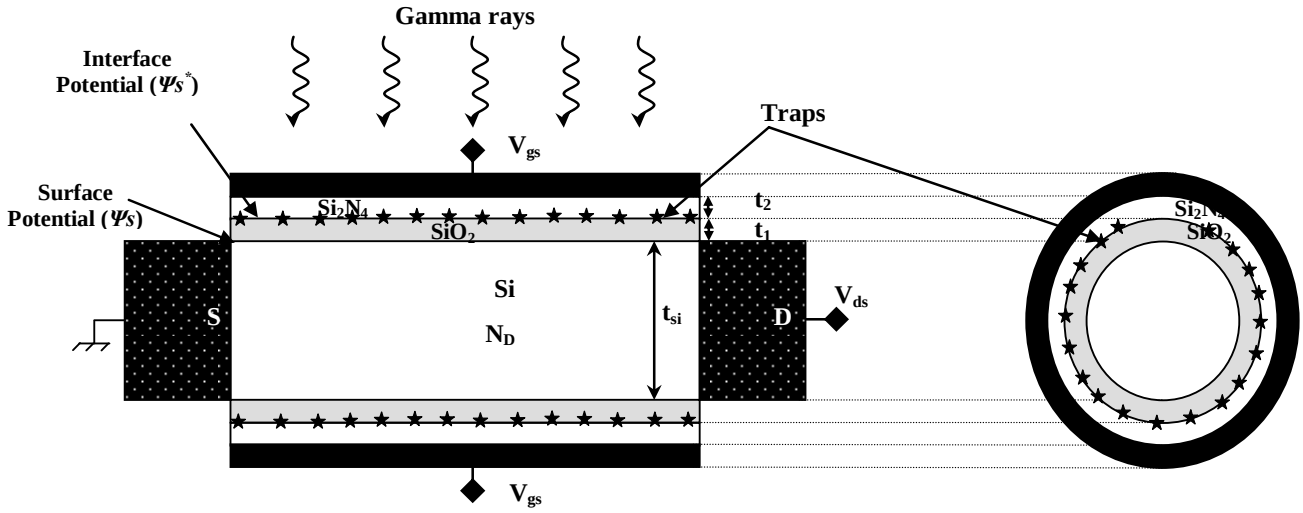

Figure 1. Cross-sectional view of the proposed DDGAA RADFET design.

drain spacing at x= 0 and L, respectively, where L is the gate length. With a negatively applied gate bias, holes generated in the SiO_2 layer are transported and trapped at the SiO_2 /Si_3N_4 interface producing a measurable threshold-voltage shift as it is shown in Fig. 1.

The investigation reported in this work for gamma radiation sources can also be applied qualitatively to other radiation sources (protons, electrons, …).

For deep submicron devices, the solution of 2D Poisson's equation satisfying suitable boundary conditions is required to model the interface potential. Refer to Fig. 1, the 2D Poisson's equation for the channel region is given by

$$\frac{1}{r}\frac{\partial}{\partial r}\left(r\frac{\partial}{\partial r}\psi(r,x)\right)+\frac{\partial^2}{\partial x^2}\psi(r,x)=\frac{q\cdot N_D}{\varepsilon_{si}} \quad (1)$$

The boundary conditions for $\psi(x,r)$ are found by satisfying continuity of both the normal component of the electric displacement at the (Si/SiO_2) interfaces, and the potential at the source/drain sides.

Using the same parabolic potential profile in vertical direction [2] and applying the symmetry condition of $\partial\psi/\partial r=0$ for $r=0$, we obtained the following expressions of 2-D channel potential as

$$\psi(r,x)=\frac{C_{ox}}{\varepsilon_{si}\cdot t_{si}}\left[V_g^*-\psi_s(x)\right]r^2+\left(1+\frac{C_{ox}t_{si}}{4\varepsilon_{si}}\right)\psi_s(x)-\frac{C_{ox}t_{si}}{4\varepsilon_{si}}V_g^* \quad (2)$$

where $\psi_s(x)$ represents the surface potential (the potential at the Si/SiO_2 interface),

with C_{ox} represents the insulator capacitance ($C_{ox}=2\pi\varepsilon_1 L/\ln(1+2t_1/t_{si})$), t_{si} is the silicon thickness, the effective oxide and silicon nitride layer is defined as $t_{oxeff}=t_1+t_2\frac{\varepsilon_1}{\varepsilon_2}$ with t_1 is the thickness of the SiO_2 ($\varepsilon_1=\varepsilon_{ox}$) layer and t_2 is the thickness of the Si_3N_4 layer (ε_2). V_{bi} is the junction voltage between the source/drain and intrinsic silicon, $V_{bi}=(kT/q)\ln(N_{D/S}/n_i)$, n_i is the intrinsic silicon density, V_{ds} represents the drain-to-source voltage and k is the Boltzmann constant. V_g^* represents the effective voltage at the gate which is introduced to simplify notations and alleviate derivations for symmetric structure as $V_g^*=V_{gs}-V_{fb}$, with V_{fb} is the flat-band voltage.

Substituting (2) in (1), we obtain the differential equation that deals only with surface potential as

$$\frac{d^2\psi_s(x)}{dx^2}-\frac{1}{\lambda^2}\psi_s(x)=D_1 \quad (3)$$

with $\lambda=\sqrt{\frac{\varepsilon_{si}\cdot t_{oxeff}\cdot t_{si}}{4\cdot\varepsilon_{ox}}}$ and $D_1=\frac{q\cdot N_D}{\varepsilon_{si}}-\frac{1}{\lambda^2}\cdot V_g^*$

where λ represents the natural length of the analyzed (DDGAA) RADFET dosimeter. This parameter gives the scaling capability (downscaling ability) of the device. D_1 is a factor which represents the impact of the applied gate voltage and channel doping on the surface potential.

The boundary conditions in channel and oxide regions (Fig.1) are given as,

$$\psi_s(x=0)=V_{bi} \quad (4a)$$

$$\psi_s(x=L)=V_{bi}+V_{ds} \quad (4b)$$

$$\varepsilon_2\frac{V_{gs}^*-\psi_s^*}{t_2}=\varepsilon_1\frac{\psi_s^*-\psi_s}{t_1} \quad (4c)$$

(continuity of the normal component of the electric displacement at the interface SiO_2 /Si_3N_4)

ISBN: 978-988-19252-1-3
ISSN: 2078-0958 (Print); ISSN: 2078-0966 (Online)

where ψ_s^* represents the interface potential at SiO_2 /Si_3N_4 interface which satisfies the continuity of the normal component of the electric displacement at the interface (Eq.(4c)).
Substituting (4c) in (3), we obtain the differential equation that deals only with interface potential as

$$\frac{d^2\psi_s^*(x)}{dx^2} - \frac{1}{\lambda^2}\psi_s^*(x) = D_2 \qquad (5)$$

with $D_2 = \alpha - \beta V_{gs}^*$ and $\alpha = \frac{qN_D\varepsilon_2 t_1}{\varepsilon_{si}(\varepsilon_2 t_1 + \varepsilon_1 t_2)}$,

$$\beta = \frac{\varepsilon_2 t_1}{\lambda^2(\varepsilon_2 t_1 + \varepsilon_1 t_2)}$$

This resolution of this Equation allows us the calculation of the interface potential without (before) irradiation.
In the case of RADFET under irradiation new term should be introduced in order to include the radiation-induced interface-traps effect [2]. So, the parameter D_2 can be written, in this case, as, $D_2 = \alpha - \beta V_{gs}^* - \frac{qN_f}{\varepsilon_2 t_2}$, with N_f represents the irradiation induced localized interface charge density per square area. The second term in this expression represents the impact of the irradiation induced localized interface charge density on the interface potential.
Using these boundary conditions (Eqs 4a, 4b and 4c), the surface and interface potentials can be, respectively, expressed as

$$\psi_S(x) = -\lambda^2 D_2 + \frac{\phi_D \sinh\left(\frac{x}{\lambda}\right) - \phi_S \sinh\left(\frac{x-L}{\lambda}\right)}{\sinh\left(\frac{L}{\lambda}\right)} \qquad (6)$$

With $\phi_D = V_{ds} + \lambda^2 D_2$ and $\phi_S = V_{bi} + \lambda^2 D_2$

$$\psi_S^*(x) = \frac{\varepsilon_1 t_2}{\varepsilon_2 t_1 + \varepsilon_1 t_2} V_{gs}^* + \frac{\varepsilon_2 t_1 x}{\varepsilon_2 t_1 + \varepsilon_1 t_2} \psi_S(x) \qquad (7)$$

B. *Threshold voltage shift model*

Schematic cross-sectional view of the proposed (DDGAA) RADFET The basic concept of RADFET dosimeter is to convert the threshold voltage shift, ΔV_{th}, induced by radiation, into absorbed radiation dose, where $\Delta V_{th} = V_{th} - V_{th0}$ with V_{th} and V_{th0} represent the threshold voltage after and before irradiation, respectively.
Based on the surface potential model given by Eq.(6), the threshold voltage can be derived using the condition of the minimum channel potential $\psi_{s\min}\big|_{V_{gs}=V_{th}} = 2.\phi_B$, with $\psi_{s\min} = \psi_s(x_{\min})$, V_{th} is the threshold voltage value, and ϕ_B represents the bulk potential of silicon body given as $\phi_B = (K_B T/q).\ln(N_D/n_i)$ where K_B represents the Boltzmann constant. The location of the minimum surface potential can be obtained analytically by solving $\frac{d\psi_s(x)}{dx} = 0$ [2].
The solution of the equation $\psi_{s\min}\big|_{V_{gs}=V_{th}} = 2.\phi_B$ at low drain-source voltage for long channel lengths (L>> λ) can be given as

$$V_{th} = \frac{\left(2A\phi_B + \lambda^2\alpha + \frac{qN_f}{\varepsilon_2 t_2}\right)\sinh\left(\frac{L}{\lambda}\right) + (V_{bi} - V_{ds})\sinh\left(\frac{L}{2\lambda}\right)}{\left(\beta\lambda^2 - \frac{B}{A}\right)\sinh\left(\frac{L}{\lambda}\right) - 2\sinh\left(\frac{L}{2\lambda}\right)} \qquad (8a)$$

with: $A = \frac{\varepsilon_1 t_2 - \varepsilon_2 t_1}{\varepsilon_1 t_2}$, $B = \frac{\varepsilon_2 t_1}{\varepsilon_1 t_2}$

$$V_{th0} = V_{th}\big|_{N_f=0} = \frac{\left(2A\phi_B + \lambda^2\alpha\right)\sinh\left(\frac{L}{\lambda}\right) + (V_{bi} - V_{ds})\sinh\left(\frac{L}{2\lambda}\right)}{\left(\beta\lambda^2 - \frac{B}{A}\right)\sinh\left(\frac{L}{\lambda}\right) - 2\sinh\left(\frac{L}{2\lambda}\right)} \qquad (8b)$$

From (8a) and (8b), the threshold voltage shift can be given as

$$\Delta V_{th} = \frac{\frac{qN_f}{\varepsilon_2 t_2}\sinh\left(\frac{L}{\lambda}\right)}{\left(\beta\lambda^2 - \frac{B}{A}\right)\sinh\left(\frac{L}{\lambda}\right) - 2\sinh\left(\frac{L}{2\lambda}\right)} \qquad (8c)$$

II. Results and Discussion

A. *Figures and Tables*

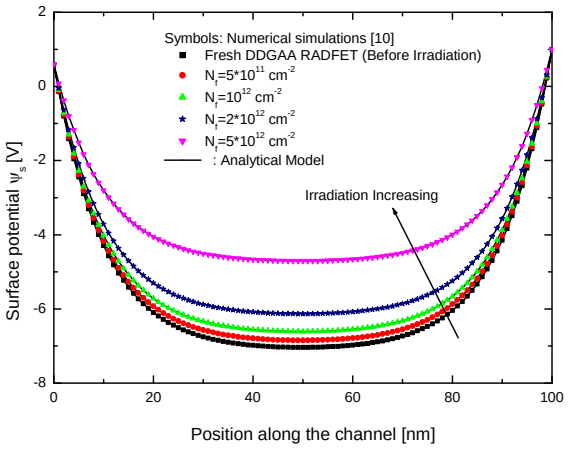

Figure 2. Variation of surface potential along the channel (b) Variation of interface potential along the SiO2/Si3N4 interface for different irradiation-induced interfacial traps densities with ($V_{gs} = -5V, V_{ds} = 1V$, $L = 100nm$, $t_1 = 5nm$, $t_2 = 5nm$, $\varepsilon_1 = 3.9$, $\varepsilon_2 = 7.5$, $t_{si} = 20nm$, $N_D = 10^{15} cm^{-3}$).

ISBN: 978-988-19252-1-3
ISSN: 2078-0958 (Print); ISSN: 2078-0966 (Online)

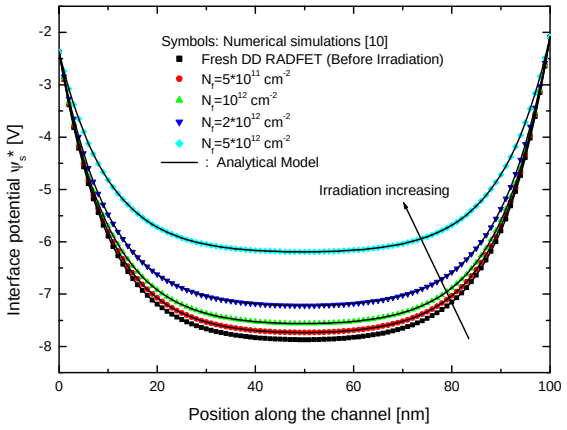

Figure 3. Threshold voltage shift variation against the irradiation-induced interfacial traps densities for the conventional and DDGAA RADFET designs.

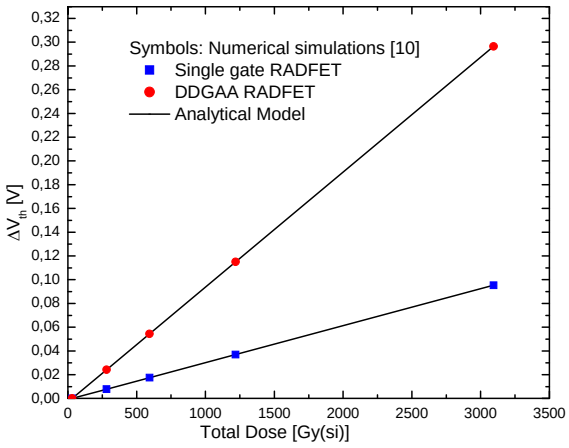

Figure 4. Variation of threshold voltage shift in function of the absorbed radiation dose for the conventional and DDGAA RADFET designs.

Figure 2 and 3 shows the variation of the calculated surface potential (Figure 2) and interface potential (Figure3) along the channel for a 100 nm DDGAA RADFET with different interface charges densities at the bias condition Vgs =-5V and Vds=1V. It can be seen that a shift (decreasing potential barrier) in the potential profile along the channel, for both surface and interface potentials, as function of the interface charges densities. The shift in the potential profile screens the region near the source end from the variations in drain voltage and thus ensures reduction in short channel effect. In addition, a good uniform increasing of the surface potential as function of the interface charge densities can be observed in Fig.2a. This surface potential behavior can provide a high threshold voltage sensitivity against the interface charges densities ( ), which is the main parameter which affects the RADFET sensitivity. Therefore, the proposed design can provide a high sensitivity performance.

The RADFET radiation sensitivity S, given by [8,9]:

$$S = \frac{\Delta V_{th}}{D} \tag{9}$$

where D represents the absorbed radiation dose.

In Figure 4, the variation of DDGAA RADFET sensitivity versus the absorbed radiation dose, D, has been compared with conventional (bulk) RADFET. For both designs, the output response of the RADFETs is linear with absorbed radiation dose. It is clearly shown that DDGAA RADFET has higher sensitivity, $S = 95.45 \mu V / Gy$, in comparison with conventional RADFET design, $S = 30.68 \mu V / Gy$. This means that DDGAA RADFET has better electrical and scaling performances in comparison with the conventional design. So, our design provides a high sensitivity, better electrical and technological performances in comparison with the conventional structure. These results make the proposed design as a promising candidate for CMOS-based dosimeters.

B. GA-based sensitivety optimisation

III. CONCLUSION

In this paper, we compared new sensor design, DDGAA RADFET, with conventional planar RADFET through 2-D analytical investigation. A two-dimensional analytical analysis comprising radiation-induced interface-traps effect, 2D surface and interface potentials, threshold voltage shift and sensitivity model for DDGAA RADFET has been developed. It has been found that incorporation of the gate all around design leads to an improvement threshold behavior while also enhancing the gate controllability, and thus provides better performance as compared to conventional planar RADFETs. The threshold voltage shift behavior of the proposed design was more effectively improved than those of the conventional planar RADFET. Also, we confirmed that DDGAA RADFET had advantages in CMOS scaling in comparison with planar RADFET. Moreover, the DDGAA RADFET has a linear sensitivity about in radiation dose ranging from D = 0 to D=3000 Gy. With continued progress towards fabricating RADFET-based dosimeters, it is possible to fabricate DDGAA RADFET without much technological processes. Our analytical analysis provides the incentive for experimental exploration of the DDGAA RADFETs with around-gate and cylindrical-channel aspects.

REFERENCES

[1] The international technology roadmap for semiconductors (ITRS); 2007. <http:// public.itrs.net>.

[2] F. Djeffal, Z. Ghoggali, Z. Dibi and N. Lakhdar, Analytical analysis of nanoscale multiple gate MOSFETs including effects of hot-carrier induced interface charges, Microelectronics Reliability, vol. 49, pp. 377-381, 2009.

ISBN: 978-988-19252-1-3
ISSN: 2078-0958 (Print); ISSN: 2078-0966 (Online)

[3] F. Djeffal , M.A. Abdi, Z. Dibi, M.Chahdi, A. Benhaya, A neural approach to study the scaling capability of the undoped Double-Gate and cylindrical Gate All Around MOSFETs, Materials Sci and Eng: B, Vol.147, pp. 239-244, 2008.

[4] H. Kaur, S. Kabra, S. Haldar and R.S. Gupta, An analytical drain current model for graded channel cylindrical/surrounding gate MOSFET, Microelectronics Journal, vol. 38, pp. 352-359, 2007.

[5] MA. Abdi , F. Djeffal, D.Arar, ML. Hafiane, Numerical analysis of Double Gate and Gate All Around MOSFETs with bulk trap states. J Mater Sci: Mater Electron, vol. 19, pp. S248-S253, 2008.

[6] A. G. Holmes-Siedle, The space charge dosimeter-General principles of a new method of radiation dosimetry, Nuclear Instruments and Methods, vol. 121, pp. 169–179, 1974.

[7] A. Kelleher, W. Lane, L. Adams, A design solution to increasing the sensitivity of pMOS dosimeters: The stacked RADFET approach, IEEE Trans. Nuclear Science, vol. 42, pp.48–51, 1995.

[8] A. Jaksic, G. Ristic, M. Pejovic, A. Mohammadzadeh, C. Sudre, W. Lane, Gamma-ray irradiation and post-irradiation responses of high dose range RADFETs, IEEE Trans. Nuclear. Science, vol. 49, pp. 1356–1363, 2002.

[9] J.R. Schwank, S.B. Roeske, D.E. Beutler, D. J. Moreno, M.R. Shaneyfelt, IEEE Trans. Nuclear Science, vol. 43, pp. 2671–2678, 1996.

[10] Atlas User's manual, SILVACO TCAD, 2008.

ISBN: 978-988-19252-1-3
ISSN: 2078-0958 (Print); ISSN: 2078-0966 (Online)